Inorg. Chem. **2009**, *48*, 2726−2728

Control of Protein Oligomerization Symmetry by Metal Coordination: C_2 and C_3 Symmetrical Assemblies through Cu^{II} and Ni^{II} Coordination

Eric N. Salgado,[†] Richard A. Lewis,[†] Susanne Mossin,[‡] Arnold L. Rheingold,[†] and F. Akif Tezcan*[,†]

Department of Chemistry and Biochemistry, University of California, San Diego, 9500 Gilman Drive, La Jolla, California 92093, and Department of Chemistry and Pharmacy, Friedrich Alexander University Erlangen-Nürnberg, Egerlandstrasse 1, 91058 Erlangen, Germany

Received January 20, 2009

We describe the metal-dependent self-assembly of symmetrical protein homooligomers from protein building blocks that feature appropriately engineered metal-chelating motifs on their surfaces. Crystallographic studies indicate that the same four-helix-bundle protein construct, MBPC-1, can self-assemble into C_2 and C_3 symmetrical assemblies dictated by Cu^{II} and Ni^{II} coordination, respectively. The symmetry inherent in metal coordination can thus be directly applied to biological self-assembly.

Homooligomeric protein complexes are believed to greatly outnumber monomeric proteins, offering such advantages as increased stability, coding efficiency, and the capacity for allostery and cooperativity.[1] The symmetry inherent in natural multiprotein assemblies also features prominently in engineered proteins and protein complexes. The symmetrical α-helical coiled-coil motif, in particular, which is utilized as a protein oligomerization unit in a myriad of cellular processes and components,[2] has been an indispensable model for the study of molecular recognition,[3] as well as the design and assembly of proteins[4] and multiprotein complexes.[5] Even in the case of such regular architectures as coiled coils, however, the prediction and control of protein oligomerization can be challenging because stable and selective protein−protein interactions (PPIs) involve large molecular surfaces. In fact, there is no canonical amino acid sequence or surface topology/makeup that will universally lead to a predictable oligomerization state. In an approach that we now call "metal-directed protein self-assembly", we have shown that a small number of metal−ligand interactions on the protein surface can be sufficiently strong to drive the self-assembly of a non-self-associating protein (MBPC-1).[6,7] If metal coordination indeed is the driving force for protein self-assembly, then, in principle, the extent and symmetry of the resulting protein superstructures should be controllable by inner-sphere metal coordination. We demonstrate here that the same protein building block oligomerizes in different symmetries, as dictated by the coordination preference of the metal ion that it associates with. Our results indicate that metal coordination can provide a modular and facile means to control symmetry in protein self-assembly.

MBPC-1 is a cytochrome cb_{562} variant, which was engineered to contain two i and $i + 4$ dihistidine motifs on the surface of Helix3 (at positions 59/63 and 73/77) for metal chelation. Upon binding of equimolar zinc, MBPC-1 was observed to form a tetrameric assembly (Zn_4:MBPC-1_4) held together by the shared coordination of four Zn ions.[6] A subsequent study indicated that salt-bridging and hydrogen-bonding interactions can dictate the geometric alignment of protein partners, leading to the population of discrete supramolecular structures over other zinc-induced conformations of similar energy. Nevertheless, the driving force for oligomer formation is provided largely, if not entirely, by zinc coordination, despite the large buried protein surface area (∼5000 Å^2).[7] Accordingly, the dihedral symmetry (D_2) of Zn_4:MBPC-1_4 is likely governed by the tetrahedral coordination environments of the four Zn ions that hold this assembly together.

In order to prove that oligomerization symmetry is indeed governed by metal coordination, we chose to establish whether the *nontetrahedral* coordination preferences of Cu^{II} and Ni^{II} could also be imposed on the symmetry of MBPC-1 self-assembly. To determine the oligomerization behavior of MBPC-1 in the presence of Cu^{II} and Ni^{II}, we obtained crystals

* To whom correspondence should be addressed. E-mail: tezcan@ucsd.edu.
[†] University of California, San Diego.
[‡] Friedrich Alexander University Erlangen-Nürnberg.

(1) Goodsell, D. S.; Olson, A. J. *Annu. Rev. Biophys. Struct.* **2000**, *29*, 105–153.
(2) Burkhard, P.; Stetefeld, J.; Strelkov, S. V. *Trends Cell. Biol.* **2001**, *11*, 82–88.
(3) Havranek, J. J.; Harbury, P. B. *Nat. Struct. Biol.* **2003**, *10*, 45–52.
(4) (a) Matzapetakis, M.; Farrer, B. T.; Weng, T. C.; Hemmingsen, L.; Penner-Hahn, J. E.; Pecoraro, V. L. *J. Am. Chem. Soc.* **2002**, *124*, 8042–8054. (b) Lombardi, A.; Summa, C. M.; Geremia, S.; Randaccio, L.; Pavone, V.; DeGrado, W. F. *Proc. Natl. Acad. Sci. U.S.A.* **2000**, *97*, 6298–6305. (c) Kharenko, O. A.; Kennedy, D. C.; Demeler, B.; Maroney, M. J.; Ogawa, M. Y. *J. Am. Chem. Soc.* **2005**, *127*, 7678–7679.
(5) Ghirlanda, G.; Lear, J. D.; Ogihara, N. L.; Eisenberg, D.; DeGrado, W. F. *J. Mol. Biol.* **2002**, *319*, 243–253.
(6) Salgado, E. N.; Faraone-Mennella, J.; Tezcan, F. A. *J. Am. Chem. Soc.* **2007**, *129*, 13374–13375.
(7) Salgado, E. N.; Lewis, R. A.; Faraone-Mennella, J.; Tezcan, F. A. *J. Am. Chem. Soc.* **2008**, *130*, 6082–6084.

10.1021/ic9001237 CCC: $40.75
Published on Web 03/06/2009

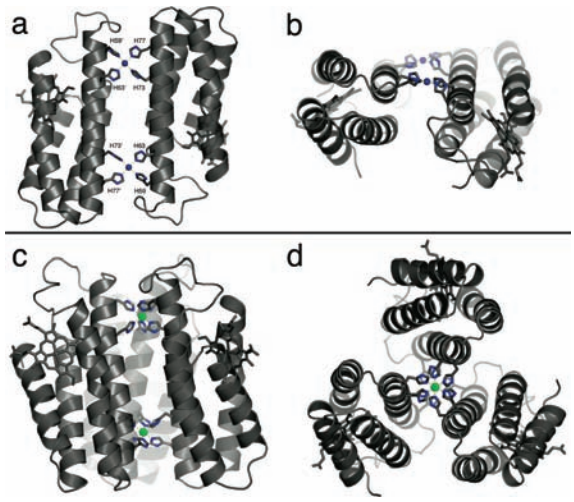

Figure 1. Ribbon representations of Cu_2:MBPC-1_2 (a and b) and Ni_2:MBPC-1_3 (c and d) crystal structures: (a and c) side views; (b and d) top views.

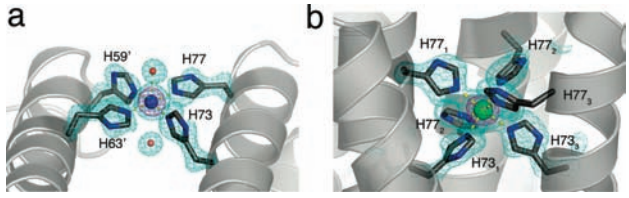

Figure 2. (a) Cu and (b) Ni coordination environments in Cu_2:MBPC-1_2 and Ni_2:MBPC-1_3 and the corresponding simulated-annealing $F_o - F_c$ omit electron density maps (cyan, 3.2σ; magenta, 8σ). Water molecules shown as red spheres (a) are positioned at 2.6 and 3.5 Å, respectively, from Cu. Axial coordination to the second water molecule is likely overcome by local electrostatic effects.

of both Cu^{II}- and Ni^{II}MBPC-1 structures and determined their structures at 1.7 and 2.0 Å resolution, respectively.

The copper assembly, Cu_2:MBPC-1_2 (PDB ID: 3DE8), is an antiparallel dimer of MBPC-1 molecules with two interfacial Cu ions that coordinate the monomers together (Figure 1a,b).[8] The Cu ions are found in a square-pyramidal coordination sphere, comprised of one His_2 motif from each monomer to form the equatorial coordination plane and an axial aquo ligand (Figure 2a).

The Cu_2:MBPC-1_2 assembly possesses an overall C_2 symmetry, with the 2-fold symmetry axis bisecting the Cu−Cu axis. The buried surface area between the monomers in both of the crystallographically distinct Cu_2:MBPC-1_2 dimers is small (800 Å^2 including the metal coordination sphere) and devoid of favorable side-chain interactions that would typically be expected to drive protein oligomerization (Table S5 in the Supporting Information).[9]

The nickel assembly, Ni_2:MBPC-1_3 (PDB ID: 3DE9), is a parallel trimer of MBPC-1 molecules held together by two Ni ions (Figure 1c,d), each coordinated octahedrally by three His_2 motifs (Figure 2b).[10] Both Ni ions are located on a crystallographic 3-fold symmetry axis in the rhombohedral crystal lattice (R_3 space group), whereby the monomeric components of Ni_2:MBPC-1_3 are interrelated by perfect 3-fold rotational symmetry (C_3; Figure 1d). As in the copper-induced dimer, protein surface interactions within Ni_2:MBPC-1_3 are minimal and nonspecific, burying only ~650 Å^2 between monomers.[9]

To further probe control of the supramolecular assembly by metal binding, which should be manifested by ideal tetragonal (Cu) or octahedral (Ni) coordination geometries, we examined in detail the coordination environments in the two structures (Figure 2). The average $Cu-N_{His}$ and $Ni-N_{His}$ distances are 2.08(3) and 2.18(6) Å, respectively, which compare well with the distances observed in the copper(II) tetrakis(*N*-methylimidazole)·$2H_2O$ [2.02(3) Å] and nickel(II) hexaimidazole [2.13(3) Å] complexes.[11,12] As expected from a Cu^{II} center, the axial aquo ligand in Cu_2:MBPC-1_2 is subject to Jahn−Teller distortion and positioned at a distance of 2.55(4) Å. The N−metal−N angles formed between His residues at cis positions are 90(2)° and 91(3)° respectively for copper and nickel species, and those between the His residues at trans positions are 178(4)° and 180(1)°, indicating near-ideal square-planar and octahedral protein−metal coordination environments. In the case of Cu_2:MBPC-1_2, the square-planar copper coordination environment is further corroborated by its axial electron paramagnetic resonance (EPR) spectrum ($S = {}^1/_2$), which is modeled well with four equivalent coordinating N ions (Figure 3). Similar to the model complexes, the histidine imidazole groups in both structures adopt a staggered arrangement, where the imidazole planes of *cis*-His residues are ~90° to one another and those of *trans*-His groups are nearly coplanar. Thus, the metal coordination environments in both assemblies appear to be uninfluenced by the supramolecular structure or any possible steric demands by the i and $i + 4$ His_2 coordination motif and the metal coordination is the primary determinant of supramolecular geometry.

To characterize the oligomerization behavior of MBPC-1 in the presence of Cu^{II} and Ni^{II} in solution, we carried out sedimentation velocity (SV) and sedimentation equilibrium (SE) experiments. Both SV and SE data confirm that copper binding exclusively leads to dimer formation at all protein concentrations tested (50−600 μM; Figures S1−S4 in the Supporting Informa-

(8) The asymmetric unit of Cu_2:MBPC-1_2 crystals contains two protein dimers, as well as six Ca ions that appear to stabilize lattice packing interactions (Figure S5 in the Supporting Information). One of these Ca ions directly bridges the two Cu_2:MBPC-1_2 assemblies in the asymmetric unit. The fact that both Cu_2:MBPC-1_2 dimers in the asymmetric unit have the same conformation (Figure 4a) despite their different modes of association with Ca ions indicates that calcium coordination does not influence the supramolecular assembly of Cu_2:MBPC-1_2.

(9) An analysis of the protein−protein interface in Cu_2:MBPC-1_2 using the PISA Server (Krissinel, E.; Henrick, K. *J. Mol. Biol.* **2007**, *372*, 774−797) indicates that the solvation free energy gain upon the formation of the interface is calculated to be only ~ −1 kcal/mol, with a Complexation Significance Score (CSS) of zero, suggesting the sidechain and mainchain interactions do not factor in the dimerization of MBPC-1. For Ni_2:MBPC-1_3, the solvation free-energy gain upon monomer−monomer docking is similarly small (−1.9 kcal/mol), with a corresponding CSS of zero (Table S6 in the Supporting Information). These findings suggest that oligomerization of MBPC-1 in both structures is driven by metal coordination.

(10) In addition, there is a weakly bound Ni ion near the N terminus of each monomer (Figure S6 in the Supporting Information). This Ni ion is internally coordinated to the N-terminal amine and the carbonyl oxygen of Ala1, Asp39, and Lys42; it is not involved in any interprotein interactions.

(11) Su, C. C.; Hwang, K. Y.; Chen, J. H.; Wang, S. L.; Liao, F. L.; Horng, J. C. *Polyhedron* **1995**, *14*, 3011–3021.

(12) Konopelski, J. P.; Reimann, C. W.; Hubbard, C. R.; Mighell, A. D.; Santoro, A. *Acta Crystallogr.* **1976**, *B32*, 2911–2913.

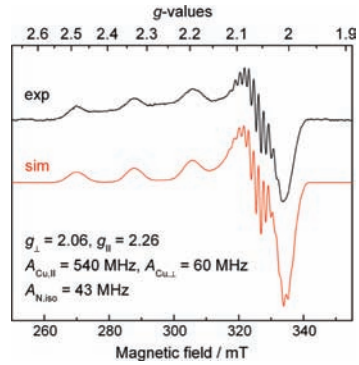

Figure 3. Experimental (black) and simulated (red) X-band EPR spectra for Cu_2:MBPC-1_2 and the parameters used for the simulation. The sample contained 1.5-fold molar excess of MBPC-1 over copper (150 vs 100 μM) to ensure that there was no free copper in solution. The data were collected at 125 K.

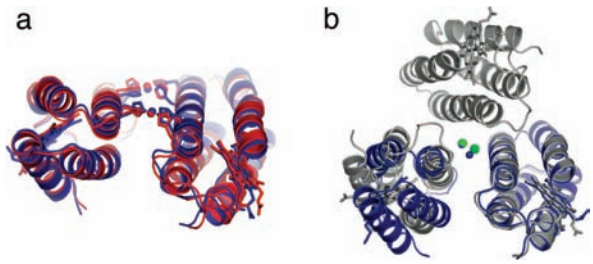

Figure 4. (a) Overlay of the two Cu_2:MBPC-1_2 assemblies in the asymmetric unit. (b) Overlay of Cu_2:MBPC-1_2 (blue) and Ni_2:MBPC-1_3 (gray) based on C_α's of a single monomeric unit. Cu and Ni ions are shown as blue and green spheres. The hinge angles between the monomeric units in both complexes were calculated as ∠[center of mass (COM) of monomer A−COM of metal ions−COM of monomer B].

tion). Interestingly, the hydrodynamic data indicate that nickel coordination also leads primarily to dimer formation at MBPC-1 concentrations that are feasible to be employed in these measurements (up to ~1 mM). Given that MBPC-1 is a non-self-interacting protein, it is likely that association of a third monomer to form the structurally characterized trimer requires high protein concentrations such as those utilized for crystallization (>4 mM).[13]

An inspection of the Cu_2:MBPC-1_2 structure invokes the possibility that there could be rotational freedom about the Cu−Cu axis to some extent. A superposition of the two Cu_2:MBPC-1_2 dimers observed in the asymmetric unit reveals that the relative orientations of the monomers in these molecules are nearly identical (root-mean-square deviation over all C_α's = 0.885 Å; Figure 4a), suggesting that the "flat" conformation of Cu_2:MBPC-1_2 likely is the preferred geometry. A further overlay of the Cu_2:MBPC-1_2 and Ni_2:MBPC-1_3 structures indicates that there is minimal difference between the hinge angles formed between individual MBPC-1 molecules in these structures (119.4° vs 120.0°; Figure 4b). On the basis of this similarity, we suggest that the dimeric species formed at intermediate nickel−protein concentrations also is a flat structure resembling Cu_2:MBPC-1_2, bearing two octahedral Ni-$His_4(H_2O)_2$ centers. Upon an increase in the MBPC-1 concentration to millimolar levels under crystallization conditions, a third MBPC-1 molecule presumably coordinates the Ni ions to yield the observed trimeric structure, which would not be favored in the case of Cu^{II} given its preference for four-coordinate geometry. It is important to note, however, that Ni ions are immediately involved in crystal packing, and therefore it is likely that formation of Ni_2:MBPC-1_3 is also favored through lattice interactions. In any case, both the C_3 trimer observed in the solid state and the dimeric, and by inference, C_2 symmetrical form observed in solution are fully compatible with the octahedral coordination preference of Ni^{II}.

In summary, the distinct MBPC-1 oligomerization geometries obtained with copper (C_2), nickel (C_3 and/or C_2), and zinc (D_2)[6] indicate that the supramolecular arrangement of this non-self-associating protein can be controlled by the metal coordination geometry, using principles commonly applied for the self-assembly of small molecules.[14] Importantly, the facile access to different symmetries through metal coordination without the need to engineer large molecular surfaces may open up the path for the construction of multidimensional protein architectures, which require building blocks that simultaneously utilize a combination of these symmetry elements.

On the basis of the observations for MBPC-1, it is tempting to suggest that any protein with metal-chelating motifs on the surface can, in principle, be treated as a large polydentate ligand, whose supramolecular arrangement can be predicted by simple coordination chemistry rules. Yet, proteins possess large, topologically complex surfaces with many functional groups, which can not only coordinate metals but also interact with one another attractively or repulsively. As we previously indicated,[7] such interactions combined can potentially lead to numerous forms of metal-mediated protein assemblies. Thus, the exclusive population of a desired superprotein architecture through metal coordination will undoubtedly require a thorough consideration of noncovalent PPIs as well as the precise localization of metal coordination.

Acknowledgment. We thank Prof. Mike Tauber, Prof. Karsten Meyer, and Hannah Shafaat for helpful discussions and experimental help. This work was supported by a Hellman Faculty Scholar Award and a Beckman Young Investigator Award (F.A.T.), the NIH (Training Grant GM08326 to E.N.S.), and the NSF (Grant 0634989 to A.L.R.). Portions of this research were carried out at the Stanford Synchrotron Radiation Laboratory, operated by Stanford University on behalf of DOE.

Supporting Information Available: Descriptions of protein expression, purification, characterization, and crystallization, as well as tables and figures for SV/SE, crystallographic data, and PPI analysis. This material is available free of charge via the Internet at http://pubs.acs.org.

IC9001237

(13) The apparent monomer−dimer association constants determined by SE measurements are 1.3×10^5 and 0.6×10^5 M^{-1} respectively for the copper- and nickel-induced dimers, consistent with the stronger coordination by Cu^{II} ions for a given ligand set.

(14) (a) Fujita, M.; Tominaga, M.; Hori, A.; Therrien, B. *Acc. Chem. Res.* **2005**, *38*, 369–378. (b) Caulder, D. L.; Raymond, K. N. *Acc. Chem. Res.* **1999**, *32*, 975–982. (c) Holliday, B. J.; Mirkin, C. A. *Angew. Chem., Int. Ed.* **2001**, *40*, 2022–2043. (d) Leininger, S.; Olenyuk, B.; Stang, P. J. *Chem. Rev.* **2000**, *100*, 853–907.